The anodic behaviour of tin and a lead–tin alloy in sulfuric acid

K. Salmi and G. Sundholm*

Helsinki University of Technology, Laboratory of Physical Chemistry and Electrochemistry, SF-02150 Espoo (Finland)

Abstract

The anodic behaviour of pure tin and a Pb–10wt.%Sn alloy have been studied in sulfuric acid solutions using the ring-disk technique and potential decay measurements. For Sn in H_2SO_4 the results show that this metal passivates partly at acid concentrations above 3 M. Tin was found to dissolve mainly as Sn(II) ions, but to some extent also as Sn(IV) if the potential is >3 V. The *ex situ* analysis of the corrosion layer formed on pure Sn showed that the layer consisted mainly of amorphous SnO. The results for the Pb–Sn alloy showed that Sn dissolves from or through the corrosion layer formed on the alloy as Sn(II) ions. Tin was found to inhibit the formation of PbO_2. The effect of Sn ions dissolved in the solution seemed to be similar to that of Sn as an alloying agent. The ring-disk voltammetric measurements showed that a tin-containing compound is formed on the Pb–Sn alloy. This product is probably a mixed Pb–Sn oxide or tin-doped PbO_n.

Introduction

The increasing use of valve-regulated lead/acid batteries, which require minimization of gassing, has resulted in an increased use of nonantimonial grid alloys, e.g., lead–calcium. In the positive plate the use of such alloys has led to passivation phenomena, possibly due to the formation of poorly-conducting oxide layers between the grid and the active mass and consequent rapid failure of the battery. It has been found [1–3] that the addition of Sn in amounts >0.2% to antimony-free and low-antimony alloys can prevent such detrimental effects on the positive plate (the 'tin effect'). We have previously studied the anodic behaviour of lead–antimony alloys in sulfuric acid and in particular the influence of antimony on the properties of the corrosion layer on lead [4, 5]; we have continued our fundamental research on the lead/acid system with an investigation of the Pb–Sn system.

In our previous work we found it beneficial to look at the corrosion of antimony itself in sulfuric acid [6–8] and we have taken the same approach for Pb–Sn. Thus we have started to study first pure Sn [9].

Recent studies of the Pb–Sn system in sulfuric acid including reviews of the earlier literature on this subject have been presented by Döring *et al.* [1, 2], Pavlov *et al.* [10] and, most recently, by Nelson and Wisdom [3] and the reader is referred to these papers for further references. From the published literature one can deduce that the mechanism of the 'tin effect' is not clear but the main mechanisms proposed range

---

*Author to whom correspondence should be addressed.

from a simple redox reaction between PbO and SnO to the formation of mixed semiconducting Pb–Sn oxides. In addition, the production process used for the grid may influence its corrosion behaviour. In this work we would like to present further results on the corrosion of Sn in sulfuric acid as well as on the corrosion of a Pb–10wt.%Sn alloy in the same medium using mainly voltammetry and the rotating disk-ring technique.

Experimental

Electrodes

Pure Pb (99.9999 wt.%) and a Pb–10wt.%Sn alloy were used as working electrodes. Depending on the type of experiment, different electrode constructions were applied. Cyclic sweeps and oxidations at constant potential succeeded by linear potential sweeps were carried out with a rotating ring-disk electrode system. The ring electrode was made of gold (99.9 wt.%). The diameter of the disk electrode was 4.7 mm and the inner and outer diameters of the ring were 5.1 and 6.0 mm, respectively. The theoretical collection efficiency for a ring-disk electrode of this geometry is 0.31. Potential decay measurements were made with a rotating disk electrode of 0.08 cm^2 geometric area.

Before each experiment, a thin layer of the electrode surface was scraped off with a scalpel and thus a clean surface was revealed. After immersing the electrode into the electrolyte it was polarized cathodically for 15 min at -1.20 V versus Hg_2SO_4/Hg (below the equilibrium potential of the $PbSO_4$/Pb couple).

Hg_2SO_4/Hg electrodes filled with cell electrolyte (measurements in 0.5 and 4.5 M acid) or with saturated K_2SO_4 (measurements in 6 M acid) were used as reference electrodes and all potentials in this paper are given versus this kind of reference electrodes. A platinum plate served as a counter electrode.

Solutions

H_2SO_4 solutions (0.5, 4.5 and 6 M) used as electrolyte were prepared from p.a. H_2SO_4 (Merck) and water purified in a Milli-Q reagent-grade water system. When studying the effect of Sn ions on the behaviour of Pb, $SnSO_4$ (Riedel de Haën AG) was dissolved in H_2SO_4. In the ring-disk experiments oxygen was removed from the solution by passing nitrogen through the cell for at least 15 min before each measurement and also during the measurement.

Equipment

The experiments were performed using a RDE4 bipotentiostat (Pine) and a PPRI waveform generator. A Varian AA975 spectrophotometer was used to determine the Sn content of solutions.

Measurements

In all measurements the rotation rate of the electrode was 1500 rpm and in the linear measurements the sweep rate was 30 mV s^{-1}.

Results and discussion

Cyclic sweep and ring-disk measurements on tin

A Sn electrode becomes partly passivated only if the concentration of sulfuric acid is higher than about 3 M. A cyclic voltammogram of Sn in 4.5 M acid is shown

in Fig. 1. When polarized in the anodic direction from about -1.10 V Sn starts to dissolve and a fairly high current density, 350 mA cm^{-2}, is reached before passivation starts (peak 1, Fig. 1) and the current density drops to quite a low value, but then increases and settles at about 70 mA cm^{-2}. Oxygen evolution starts above 3.5 V. The cathodic sweep in 4.5 M acid shows one reproducible peak, 6 in Fig. 1. We have shown [9] that this peak, which is due to a surface process, is connected to the anodic peak 1.

In 6 M acid, Fig. 2(a), the cyclic voltammogram looks much the same as in 4.5 M H$_2$SO$_4$, but the current in the partly passive region is lower, about 25 mA cm^{-2}, and in the cathodic sweep a new, reproducible peak, 5 in Fig. 2(a) appears.

The ring-disk experiments (Fig. 2(a–c)) shows that when the gold ring electrode is polarized so that any Sn(II) species dissolved from the disk are oxidized on the ring the resulting ring current during the cyclic sweep of the disk looks like in Fig. 2(b), E(Sn(II)/Sn = -0.748 V [11]). Detection of Sn(IV) independently of Sn(II) can be achieved by polarizing the ring to a potential below that of the equilibrium potential of the system Sn(IV)/Sn(II), which is -0.458 V [11], but above that of hydrogen evolution on gold. The result of such a measurement is shown in Fig. 2(c).

The results of these ring-disk measurements show, Figs. 2(a, b), that Sn dissolves mainly as Sn(II) both in the active and the partly passive potential region up to the start of oxygen evolution. During the cathodic sweep the ring current is quite constant, which means that Sn dissolves at a constant rate through the anodic film formed at potentials > -0.8 V.

In contrast, as seen by comparing Figs. 2(a and c), Sn does not dissolve as Sn(IV) during the anodic-going sweep. At potentials >3 V a cathodic ring current appears. This is probably caused mainly by reduction of oxygen, which starts to evolve on the disk at this potential. (Oxygen is reduced on gold if the potential is ≤ -0.10 V [12]).
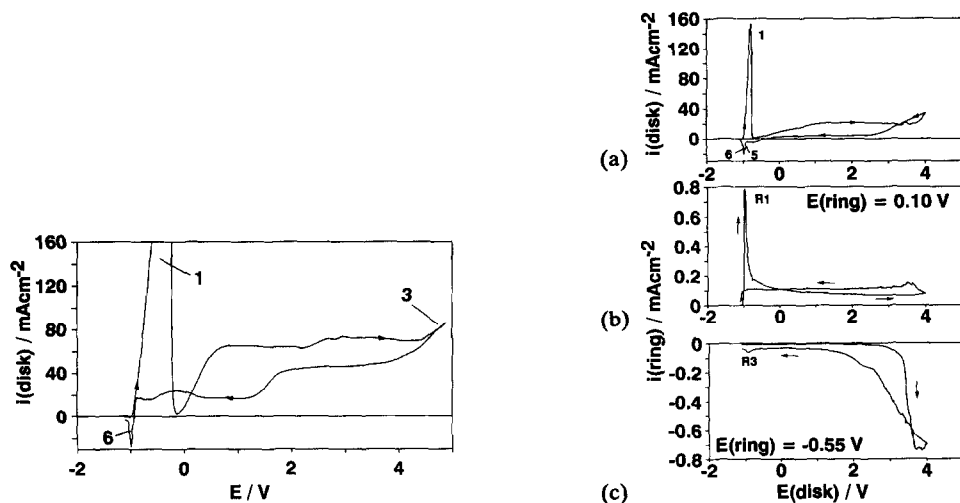

Fig. 1. Cyclic voltammogram of a tin disk electrode in 4.5 M sulfuric acid solution (sweep rate 30 mV s^{-1} and the rotation rate of the electrode 1500 rpm).

Fig. 2. The ring-disk voltammogram of the gold ring/Sn disk electrode in 6 M H$_2$SO$_4$: (a) disk voltammogram, (b) current of the ring polarized to 0.10 V, and (c) current of the ring polarized to -0.55 V (sweep rate and rotation rate as in Fig. 1).

On the cathodic sweep a reproducible ring peak, R3 in Fig. 2(c), which corresponds to peak 5 on the disk voltammogram, Fig. 2(a), appears. Peak R3 is seen only if the anodic potential of the disk is >3.5 V and the acid concentration is >4.5 M. This indicates that some Sn(IV) species dissolve when the corrosion film on Sn is reduced, but only if the film is formed at high anodic potentials.

Cyclic sweep and ring-disk measurements on Pb–10wt.%Sn

Cyclic sweep measurements were started from a potential of − 1.20 V. A typical result in 4.5 M H_2SO_4 is shown in Fig. 3, where the corresponding measurement on pure Pb is included for comparison. (For peak notations and interpretations concerning Pb and Pb–10wt.%Sn see Table 1). On the anodic going sweep Pb is oxidized to $PbSO_4$, peak A1, and after this a peak, A13 in Fig. 3, appears, the potential of which corresponds to that of peak 1 (Figs. 1, 2(a)) observed on pure Sn. It is thus due to the dissolution of Sn, probably as Sn(II). This oxidation peak has also been observed by Ijomah [13] and Döring et al. [1]. In the passive region a hump is seen, evidently due to increased dissolution of Sn. This feature, as well as peak A13, disappears at higher concentrations of acid. An inspection of the oxygen evolution region (A2, Fig. 3), shows that this reaction occurs with a higher overpotential on the alloy than on Pb.

On the cathodic sweep the Pb–Sn system shows an additional reduction peak, compared to Pb, C14 at about − 0.7 V, tentatively assigned to the reduction of Sn ions. Our interpretation of the reactions corresponding to the cathodic peaks C8 and C14 differs from that of Ijomah [13], who assumes the reverse order for the assignment of these two current peaks. Our conclusion is based on a careful comparison of the voltammograms of Pb and the Pb–Sn alloy. Both in 0.5 M and 4.5 M H_2SO_4 C8, corresponding to reduction of PbO (and higher oxides of Pb [4]), has a peak potential
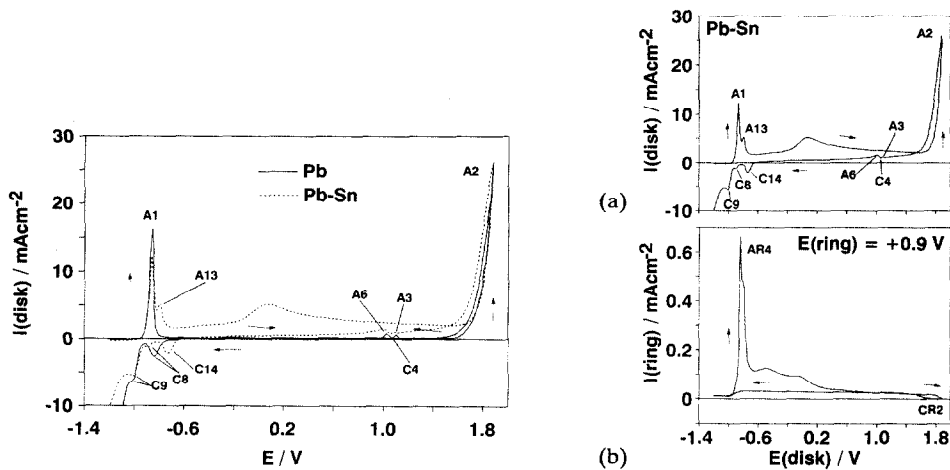

Fig. 3. Cyclic voltammograms of a Pb (solid line) and a Sn disk (dashed line) in 4.5 M H_2SO_4 (sweep rate and rotation rate as in Fig. 1).

Fig. 4. The cyclic ring-disk voltammogram of the gold ring/Pb–Sn disk electrode in 4.5 M H_2SO_4: (a) disk voltammogram, (b) current of the ring polarized to + 0.9 V (sweep rate and rotation rate as in Fig. 1).

TABLE 1

The notations and interpretations of the current peaks observed in the ring-disk voltammetric experiments on Pb and the Pb–Sn alloy (A - anodic, C - cathodic current)

Disk		
A1		Formation of divalent Pb and deposition of $PbSO_4$
A2		Formation of tetravalent oxides of Pb (PbO_n, PbO_{2-x}, PbO_2)
A3 and A6		Oxidation of metallic Pb substrate and/or incompletely oxidized products of Pb
Al3		Formation of divalent Sn and deposition of a divalent product of Sn
C4		Reduction of tetravalent oxides of Pb
C8		Reduction of PbO and tetravalent products of Pb
C9		Reduction of $PbSO_4$ to Pb
C14		Reduction of Sn compound
C15		Reduction of Sn-containing compound
Ring		
AR4-AR6		Oxidation of Sn(II) ions to Sn(IV)
CR2-CR7		Reduction of Pb(IV) ions to Pb(II)

of about -0.84 V on Pb and -0.88 V on Pb–Sn, whereas the peak potential of C14 is always higher than -0.8 V.

Due to the interaction of the redox systems of Pb and those of Sn it is difficult to study the dissolution of Sn from the Pb–Sn alloy as Sn(IV), but the dissolution of Sn as Sn(II) can be followed by polarizing a gold ring electrode at a potential just below that of the equilibrium potential of the system $PbO_2/PbSO_4$ (1.10 V in 4.5 M H_2SO_4). The only possible interference with the anodic reaction Sn(II) $\rightarrow$ Sn(IV) on the ring could thus be from the cathodic reaction Pb(IV) $\rightarrow$ Pb(II)). In Fig. 4(a, b) we show the result of a ring-disk electrode measurement in 4.5 M acid with the ring polarized to $+0.90$ V. The ring current curve shows that Sn dissolves from the Pb–Sn alloy as Sn(II) as soon as $PbSO_4$ starts to form (peak AR4, Fig. 4(b)). The dissolution rate diminishes gradually. At a potential >1.5 V a small cathodic current, CR2, appears. This is due to the dissolution of some Pb as Pb(IV) ions. On the cathodic sweep dissolution of Sn through the corrosion layer continues at a steady rate until a potential corresponding to reduction of $PbSO_4$ on the disk is reached. No increase in the dissolution of Sn as Sn(II) can be seen corresponding to peak C14 at -0.7 V on the disk, which indicates that reduction of Sn from the anodic oxide layer on Pb–Sn is mainly a solid-state process.

Results of the cathodic reduction of the oxide layer formed at constant potential on Pb–10wt.%Sn

For further characterization of the differences between pure Pb and the Sn alloy an oxide film was formed on the Pb–Sn disk electrode by polarization at constant potential in the PbO_2 region for different periods of time. A linear potential sweep in the cathodic direction was then applied and the current/potential curve of the disk electrode registered. At the same time the current at the gold ring electrode, held at a constant potential, could also be registered as a function of the potential of the disk.

The voltammogram of the Pb–Sn electrode after oxidation at a constant potential of 1.10 V in 0.5 M and 1.40 V in 4.5 M H_2SO_4 using two different oxidation times is shown in Figs. 5 and 6. In addition to the reduction peaks of PbO_2(C4), of Pb
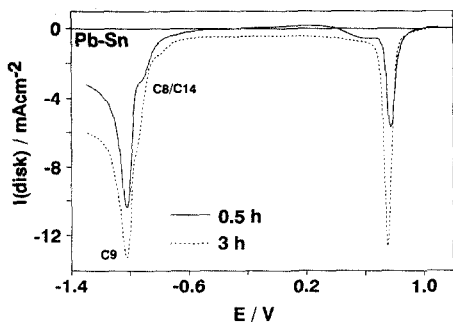
Fig. 5. The voltammogram of the Pb–Sn disk electrode succeeding an oxidation for 0.5 h (solid line) and 3 h (dashed line) at 1.1 V in 0.5 M H_2SO_4 (sweep rate and rotation rate as in Fig. 1).
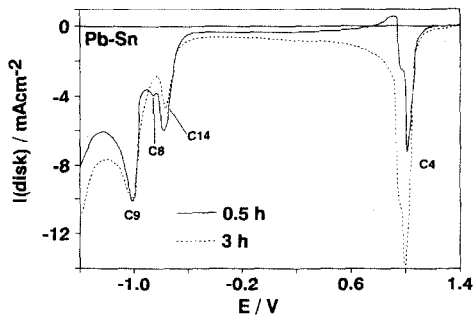
Fig. 6. The voltammogram of the Pb–Sn disk electrode succeeding an oxidation for 0.5 h (solid line) and 3 h (dashed line) at 1.4 V in 4.5 M H_2SO_4 (sweep rate and rotation rate as in Fig. 1).
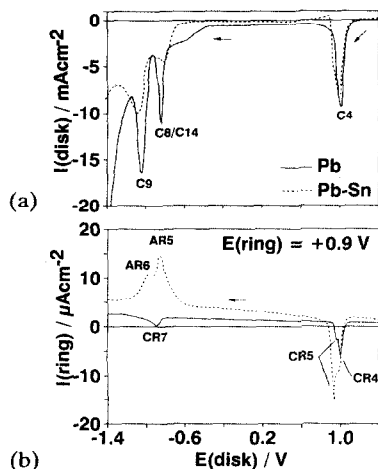

Fig. 7. The ring-disk voltammograms of the gold ring/Pb disk (solid line) and gold ring/Pb–Sn disk electrode (dashed line) succeeding an oxidation for 1 h at 1.4 V in 4.5 M H_2SO_4: (a) disk voltammogram, (b) current of the ring polarized to +0.9 V (sweep rate and rotation rate as in Fig. 1).

and/or some Pb oxides with a higher oxidation state of Pb than II(C8) and $PbSO_4$ (C9), the voltammograms of the Pb–Sn alloy in 0.5 M acid show a broad reduction peak (C15, Fig. 5), which disappears if the oxidation time at 1.40 V is increased above 1 h or the concentration of acid is increased above 3 M. Peak C14, assigned to the reduction of Sn ions, is seen on the cathodic voltammogram of the alloy, Fig. 6, only if the anodic potential is above 1.00 V and the acid concentration is above 3 M. The peak potential is about −0.75 V under the measurement conditions we have used. A further comparison of the cathodic voltammograms of Pb and the Pb–Sn alloy (see Fig. 7(a)) shows that peaks C4, C8 and C9 are all higher on Pb than on the alloy

under otherwise identical conditions. This indicates that less oxide is formed at constant potential on Pb–Sn than on Pb.

During the cathodic potential sweep of the disk electrode the gold ring electrode was polarized to 0.90 V, which enabled the detection of the dissolution of Sn as Sn(II) from the alloy electrode. The result, Figs. 7(a, b), show that at the potential where PbO_2 is reduced (C4) on the disk two cathodic peaks, CR4 and CR5 in Fig. 7(b), are seen on the ring. Thus reduction of PbO_2 to $PbSO_4$ occurs as a dissolution-precipitation reaction on the Pb–Sn alloy, with the release of Pb(IV) ions (and perhaps Pb(III)) into the solution [4]. On the ring electrode two broad anodic current peaks, AR5 and AR6 in Fig. 7(b), appear in the potential range -0.6 to -1.2 V. They are absent when Pb is used as the disk electrode and are evidently due to the oxidation of Sn(II) ions released in this potential range during the reduction of the oxide layer formed on Pb–Sn. The appearance of two peaks, AR5 and AR6, may be due to some simultaneous reduction of Pb(IV). The ring current shows that some lead Pb(IV) ions are released in this potential range, Fig. 7(b). If the oxidation time of the disk electrode is increased the ring peaks AR5 and AR6 grow, which indicates that the Sn content of the oxide layer grows with time. A lowering of the oxidation potential in the PbO_2 region has the same effect. This would indicate that more Sn is able to pass into solution when the dioxide layer is thinner. The broadness of the potential range where Sn is observed to dissolve as Sn(II) on the other hand points to the fact that the oxide layer does not contain simple Sn oxide but rather Pb–Sn mixed oxides.

Potential decay measurements

The open-circuit potential decay curves of a rotating Pb and Pb–Sn electrode after oxidation for 2 min at 1.7 V in 4.5 M H_2SO_4 are shown in Fig. 8. On Pb an initial fast potential decay is followed by a plateau due to the dissolution (self-discharge) of PbO_2. After this arrest the potential of the Pb electrode drops again. On Pb–Sn the plateau due to dissolution of PbO_2 is of much shorter duration. This result, supported by the results obtained above from a comparison of the cathodic voltammograms of Pb and Pb–Sn, suggests that Sn has an inhibiting effect on the formation of PbO_2 during the early stages of oxidation of Pb.
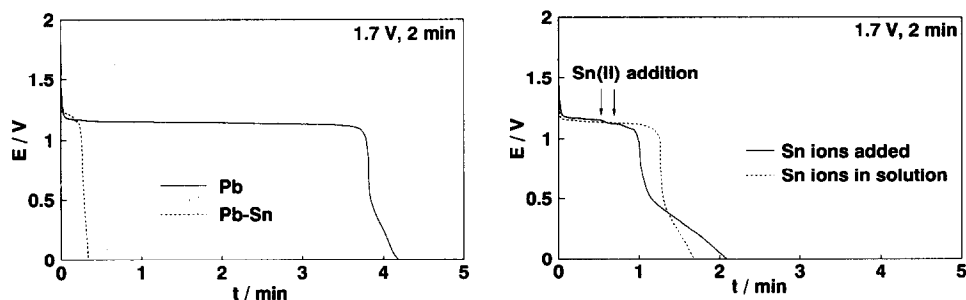

Fig. 8. The potential decay curve of the Pb (solid line) and the Pb–Sn electrode (dashed line) after an oxidation for 2 min at 1.7 V in 4.5 M H_2SO_4 (rotation rate of the electrode 1500 rpm).

Fig. 9. The potential decay curve of the Pb electrode after an oxidation for 2 min at 1.7 V in 4.5 M H_2SO_4. Solid line: acid containing Sn(II) ions were added to the electrolyte in the very beginning of the potential decay (range of addition marked with arrows; final concentration of Sn ions 130 mg l^{-1}). Dashed line: the oxidation and the decay measured in acid containing 130 mg l^{-1} Sn ions (rotation rate of the electrode 1500 rpm).

The influence of Sn(II) ions in solution on the oxidation of a Pb electrode was studied by either adding 130 mg/l Sn(II) to the solution at the start of the experiment or just at the beginning of the open-circuit potential decay. The result, given in Fig. 9, shows that Sn ions in the solutions reduce the duration of the plateau for dissolution (self-discharge) of PbO_2 on lead. This effect must be due to an adsorption of Sn(II) ions on PbO_2 in the same way as has been deduced for the similar effect of antimony ions [4].

Conclusions

The results of the experimental work regarding oxidation of Sn in H_2SO_4 shows that partial passivation of this metal occurs if the acid concentration is above 3 M. Anodic dissolution occurs mainly as Sn(II) ions. Sn(IV) ions appear if the potential is ≥ 3 V. As confirmed by surface analysis [9] the oxide film is mainly based on SnO although higher oxidation states of Sn can be present in the solid state, at least at high anodic potentials.

The results presented for the Pb–10wt.%Sn alloy are to some extent preliminary. They indicate, however, that also from the alloy Sn is released mainly as Sn(II) ions from or through the oxide film. PbO_2 formation seems to be inhibited in the presence of Sn. In fact, addition of Sn(II) ions to the acid solution seems to have the same effect on the oxide film as Sn as an alloying agent. The voltammetric results together with the ring-disk measurements indicate that mixed, probably semiconducting Pb–Sn oxides or highly tin-doped PbO_n are formed on the alloy in accordance with the suggestions of Pavlov et al. [10] and Döring et al. [1, 2].

References

1 H. Döring, J. Garche, W. Fischer and K. Wiesener, H. *J. Power Sources, 28* (1989) 367.
2 H. Döring, J. Garche, H. Dietz and K. Wiesener, *J. Power Sources, 30* (1990) 41.
3 R. F. Nelson and D. M. Wisdom, *J. Power Sources, 33* (1991) 165.
4 T. Laitinen, K. Salmi, G. Sundholm, B. Monahov and D. Pavlov, *Electrochim. Acta, 36* (1991) 605.
5 D. Pavlov, B. Monahov, G. Sundholm and T. Laitinen, *J. Electroanal. Chem., 305* (1991) 57.
6 D. Pavlov, M. Bojinov, T. Laitinen and G. Sundholm, *Electrochim. Acta, 36* (1991) 2081.
7 D. Pavlov, M. Bojinov, T. Laitinen and G. Sundholm, *Electrochim. Acta, 36* (1991) 2087.
8 T. Laitinen, H. Revitzer, G. Sundholm, J. Vilhunen, D. Pavlov and M. Bojinov, *Electrochim. Acta, 36* (1991) 2093.
9 T. Laitinen, K. Salmi, G. Sundholm, P. Viinikka and A. Yli-Pentti, *Electrochim. Acta, 37* (1992) 1797.
10 D. Pavlov, B. Monahov, M. Maja and N. Penazzi, *J. Electrochem. Soc., 136* (1989) 27.
11 B. N. Stirrup and N. A. Hampson, *Surf. Technol., 5* (1977) 429.
12 S. Laihonen, T. Laitinen, G. Sundholm and A. Yli-Pentti, *Electrochim. Acta, 35* (1990) 229.
13 M. N. C. Ijomah, *J. Appl. Electrochem., 18* (1988) 142.